



Contents lists available at ScienceDirect

Optik

journal homepage: www.elsevier.com/locate/ijleo

Original research article

Characteristic research of uniform-doping and exponential-doping $\text{Ga}_{1-x}\text{Al}_x\text{As}/\text{GaAs}$ photocathode with femtosecond laser illumination

Shalu Zhu^a, Liang Chen^{a,b,*}, Yunshen Qian^b, Hemang Jani^c, Lingze Duan^c^a Institute of Optoelectronics Technology, China Jiliang University, 310018, Hangzhou, China^b Institute of Electronics Engineering & Optoelectronics Technology, Nanjing University of Science and Technology, 210094, Nanjing, China^c Department of physics, the University of Alabama in Huntsville, 35899, Huntsville, USA

ARTICLE INFO

Keywords:

$\text{Ga}_{1-x}\text{Al}_x\text{As}$
GaAs
Photocathode
Energy band gap
Electronic optical property
Femtosecond laser
Transient property
Reflectivity

ABSTRACT

The properties and characteristics of graded Al component $\text{Ga}_{1-x}\text{Al}_x\text{As}/\text{GaAs}$ photocathode are investigated in this paper, especially the transient reflectivity of $\text{Ga}_{0.37}\text{Al}_{0.63}\text{As}$ under the condition of femtosecond laser illumination. Using software CASTEP, we calculate and analyze the optoelectronic property of varied Al composition $\text{Ga}_{1-x}\text{Al}_x\text{As}$ photocathode based on first principle theory. $\text{Ga}_{0.37}\text{Al}_{0.63}\text{As}$ is emphasized studied because its lattice constant is very close to GaAs, reducing the probability of lattice mismatch and the back interface recombination velocity on the interface of substrate and emission layer. In this work, we design two reflection mode GaAs photocathode samples with different doping method: uniform-doping and exponential-doping used in emission layer grown by MBE. The impacts of different doping method on photocathode are analyzed by comparing some typical performance parameters. Transient reflectivity rates of different doping method $\text{Ga}_{1-x}\text{Al}_x\text{As}/\text{GaAs}$ photocathode are investigated by the device of pump-probe transient reflectivity system in the paper and we found that the way of exponential-doping is better for improving the performance of $\text{Ga}_{1-x}\text{Al}_x\text{As}/\text{GaAs}$ photocathode. The potential value of transient property of photocathode is enormous in future.

1. Introduction

Negative-electron-affinity semiconductor photocathode is mostly applied in ultraviolet detection, photon-enhanced emission tube and night vision area, etc. NEA GaAlAs photocathode has widespread application in infrared detection, night vision image intensifier, and polarized electron sources due to their high quantum efficiency and low thermal emittance [1–4]. The quantum efficiency is the key standard to value the performance of photocathode, which mainly depends on the key parameters such as: the electron diffusion length (L_D), the back interface recombination velocity (S_V), and the surface escape probability (P) [5]. Al constituent can adjust the band gap and spectral response range of GaAs photocathode. NEA GaAlAs photocathode has broad prospect in the wide regions such as: undersea exploration, ocean detection, deserts and atmosphere measurement.

In this paper, the energy band and absorption of $\text{Ga}_{1-x}\text{Al}_x\text{As}$ with Al constituent of $x = 0$, $x = 0.25$, $x = 0.63$ and $x = 1$ are calculated by means of Material Studio Software. In the experiment, we choose GaAs as the study object for researching the effect of different doping method on photocathode. Two types of r-mode GaAs photocathode samples are both grown by MBE and the epitaxial

* Corresponding author at: Institute of Optoelectronics Technology, China Jiliang University, 310018, Hangzhou, China.
E-mail address: 2686084732@qq.com (L. Chen).

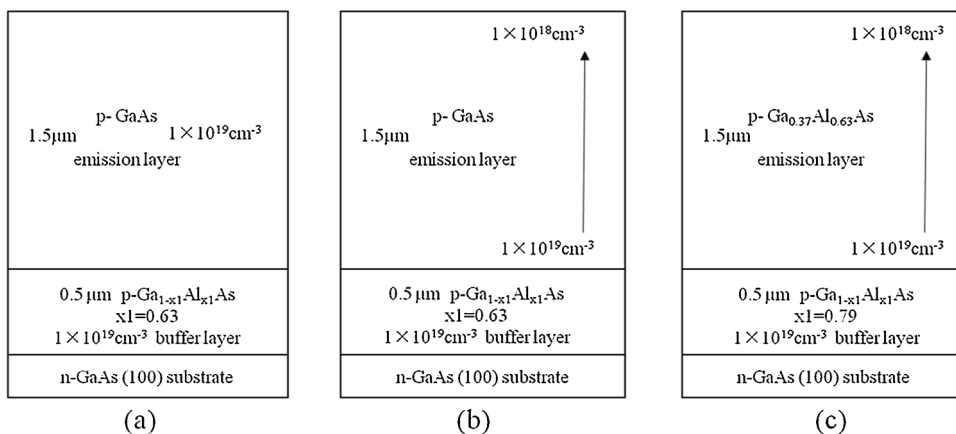


Fig. 1. Structure diagram of r-mode NEA Ga_{1-x}Al_xAs photocathode. (a) Sample 1: uniform-doping GaAs photocathode. (b) Sample 2: exponential-doping GaAs photocathode. (c) Sample 3: exponential-doping Ga_{0.37}Al_{0.63}As photocathode.

layers are doped by uniform-doping method and exponential-doping method respectively. The electron diffusion length (L_D), the back interface recombination velocity (S_V), the surface escape probability (P) and quantum efficiency (η) under the different doping condition are fitted and analyzed.

Meanwhile, we choose Ga_{0.37}Al_{0.63}As with Al constituent participation as one of study object in femtosecond transient measurement experiment for researching the transient dynamic phenomenon. Transient reflectivity rate of two kinds of r-mode Ga_{1-x}Al_xAs photocathode (exponential doping r-mode Ga_{0.37}Al_{0.63}As photocathode and uniform doping GaAs photocathode) measured by the device of pump-probe transient reflectivity system. The exponential doping r-mode Ga_{0.37}Al_{0.63}As photocathode and uniform doping GaAs photocathode is illuminated by femtosecond laser respectively for observing the transient optical property of photocathode and researching the impact of different doping method for transient dynamics. These research results can help to optimize the structure design and contribute to the deeper understanding of the carrier dynamics mechanism in the photocathode.

2. Calculation and experiment

2.1. Photocathode preparation

Firstly, we design two identical reflection mode GaAs photocathode samples using uniform-doping method and exponential-doping method respectively [12–15]. 2-in-diameter reflection mode GaAs grown by MBE is made from high-quality n-type GaAs (100) oriented substrate layer, 0.5 μm p-type zinc(Zn)-doped Ga_{0.37}Al_{0.63}As buffer layer and 1.5 μm p-type GaAs emission layer. The doping method of one of GaAs photocathode in emission layer is uniform-doping method named as sample 1 and the doping concentration in emission layer is $1 \times 10^{19} \text{cm}^{-3}$ as well as in buffer layer. Exponential-doping in emission layer of another GaAs photocathode, which doping concentration varies from $1 \times 10^{19} \text{cm}^{-3}$ to $1 \times 10^{18} \text{cm}^{-3}$ from the bottom emission layer to the surface, is named as sample 2. The two photocathode structures are shown in Fig. 1(a) and (b) respectively.

2.2. Pump-probe transient reflectivity system

We grow Ga_{1-x}Al_xAs at Al constituent $x = 0.63$ photocathode Ga_{0.37}Al_{0.63}As photocathode with exponential doping method named as sample 3. The exponential-doping Ga_{0.37}Al_{0.63}As photocathode structure is shown in Fig. 1(c).

For studying ultrafast transient carrier dynamics in uniform-doping r-mode GaAs (sample 1) and exponential-doping r-mode Ga_{0.37}Al_{0.63}As (sample 3), we design a broadband pump-probe transient reflectivity system by means of femtosecond time-resolved measurement [16].

As shown in Fig. 2, the broadband pump-probe transient reflectivity system completely consists of light source (a sub-8-fs Ti: Sapphire laser), reflecting mirror (M), Dispersion-compensating mirror (DCM) pair, beam-splitter (BS), chopper, lens, polarizer, detector, lock-in amplifier and computer (not drawn in Fig. 4). In our experiment, the broadband pump-probe transient reflectivity system has about 300 nm spectral coverage and the light source generates 540-mW average power at an 83 MHz repetition rate. Dispersion caused by air and all optics during beam transportation must be balanced by using of DCM pair and it is minimized by adopting an all-reflective beam path. A broadband beam-splitter (BS) is used to split laser beam to equal amount of pump beam and probe beam. An optical component chopper chops the pump beam at 1.9 KHz. The optical delay line (blue dashed line rectangular) is controlled by stepper motor to control optical path difference (OPD) for achieving alterable delay time Δt . Pump beam has larger average power and is incident on the sample near normal direction passing through a lens. Probe beam has weaker average power and is focused onto the sample at an incident angle approximate 16° . Reflected probe beam passing through a polarizer for eliminating the influence of scattered pump light is incident into the detector. Substantially, the detector output feed into lock-in amplifier to amplify the intensity change of probe beam caused by pump beam (Pump beam worked on the sample will change the surface

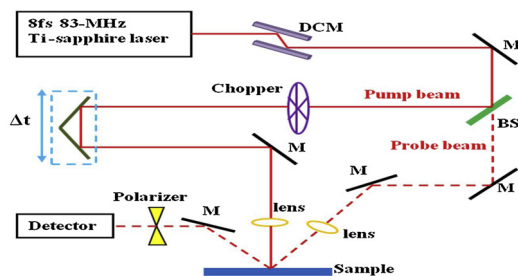


Fig. 2. Layout of broadband pump-probe transient reflectivity system.

M: reflective mirror, BS: beam-splitter, DCM: Dispersion-compensating mirror.

property of sample resulting to intensity of probe light changing). Finally, the experiment data of transient reflectivity rate verses delay time of sample 1 and sample 3 will be analyzed by computer.

3. Results and analysis

3.1. Optoelectronic properties of $Ga_{1-x}Al_xAs$

Optoelectronic properties calculation is performed by the quantum mechanics program Cambridge Serial Total Energy Package (CASTEP) [6–8] based on the first principle density function theory (DFT). The Broyden-Fletcher-Goldfarb-Shanno (BFGS) algorithm is to optimize the $Ga_{1-x}Al_xAs$ models and the plane-wave pseudo-potential method based on DFT within the generalized-gradient approximation (GGA) [9] is used in calculation. During CASTEP calculation, band structure of $Ga_{1-x}Al_xAs$ models is obtained. As we all know, GaAs is direct band gap material, but AlAs is indirect band gap material. When x is in the range of 0 to 0.45 [17], the $Ga_{1-x}Al_xAs$ is direct band gap. Otherwise, it's indirect band gap. The theoretical formula of $Ga_{1-x}Al_xAs$ material energy gap is [17]:

$$E_g(x) = \begin{cases} 1.424 + 1.247x & x < 0.45 \\ 1.9 + 0.125x + 0.143x^2 & x > 0.45 \end{cases} \quad (1.1)$$

The results of calculated band gap and theoretical band gap of $Ga_{1-x}Al_xAs$ at $x = 0, 0.25, 0.63$ and 1 are shown in Table 1. As shown in Table 1, the calculated values are lower than theoretical. It is because the DFT in calculation is ground state theory while the energy gap belongs to excited [17]. The band structure of $Ga_{1-x}Al_xAs$ at Al constituent $x = 0$ and 0.63 are shown in Fig. 3.

Absorption coefficient represents the ability of photocathode absorbing light. It can be described as the percentage of the light intensity decays transporting unit distance [10,11]. Adsorption spectra of $Ga_{1-x}Al_xAs$ with different Al constituent can be expressed by:

$$\alpha = \frac{2\omega k}{c} = \frac{4\pi k}{\lambda_0} \quad (1.2)$$

The absorption coefficient arrives at the peak when the wavelength of incident light photon is 155 nm and the wavelength range of high absorption coefficient is 100 nm–500 nm. The results are shown in Fig. 4 in detail.

Moreover, according the calculation results in Table 1, the absorption peaks of $Ga_{1-x}Al_xAs$ move towards higher incident photon energy side (lower wavelength) with Al constituent increasing. It is because the atomic radius of Al is smaller than Ga. The attractive force between atomic nucleus and outer shell electron of Al is stronger than that of the Ga [17]. Therefore, the energy used to excite the electrons become higher.

3.2. Performance characteristics comparison of uniform-doping GaAs photocathode and exponential-doping GaAs photocathode

We measure the quantum efficiency of uniform-doping GaAs NEA photocathode (sample 1) and exponential-doping GaAs NEA photocathode (sample 2) by online utilizing the multi-information measurement system [19] designed by Nanjing University Science and Technology. Quantum efficiency of the two samples is shown in Fig. 5.

The performance parameters are obtained by fitting the quantum efficiency formula from Ref. [19]. The fitting method of

Table 1
Band gap of $Ga_{1-x}Al_xAs$.

Al constituent x	0	0.25	0.63	1
Calculated value (eV)	0.521	0.857	0.917	1.374
Theoretical value (eV)	1.424	1.736	2.035	2.168
Absorption peak (10^3 cm^{-1}) photon energy(eV)	32.9	33.2	33.1	33.5
	6.47	6.8	6.93	6.96

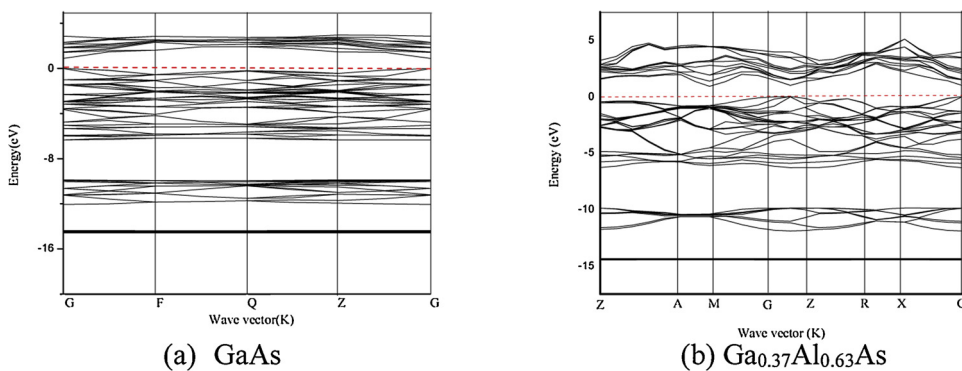


Fig. 3. Energy band structure of GaAs and Ga_{0.37}Al_{0.63}As.

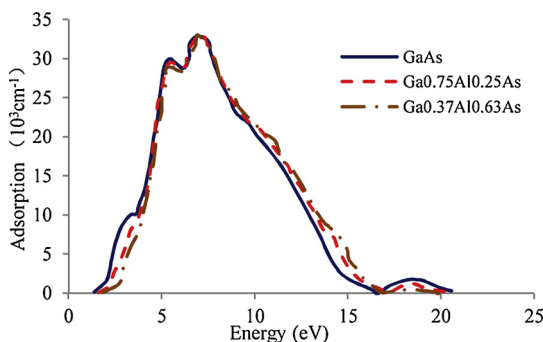


Fig. 4. Adsorption spectra of Ga_{1-x}Al_xAs.

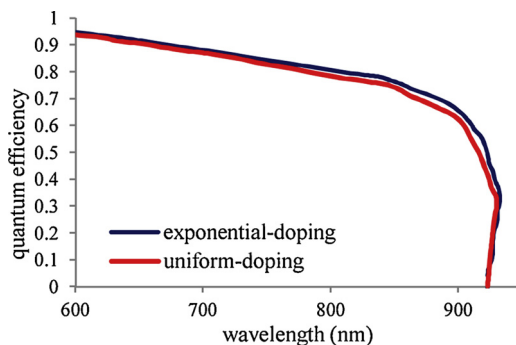


Fig. 5. Quantum efficiency of uniform-doping r-mode GaAs photocathode (sample 1) and exponential-doping r-mode GaAs photocathode (sample 2).

uniform-doping and exponential-doping r-mode GaAs employs least square method. Fitting results of performance parameters are shown in Table 2.

As it can be seen from above results, the exponential-doping method is better for photocathode performance than uniform-doping method. L_D , P of sample 2 is higher than sample 1, and we found that the doping method would affect back interface velocity S_v . S_v of exponential-doping is smaller than uniform-doping and it also contributes to the improvement of escape probability P of electrons.

Table 2
performance parameters of sample 1 and sample 2.

GaAs photocathode	L_D (μm)	S_v (cm/s)	P
Uniform-doping	1.2	1.3×10^6	0.52
Exponential-doping	2.3	1×10^6	0.53

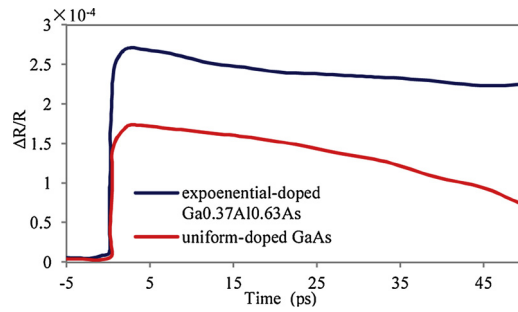


Fig. 6. Transient reflectivity rate of exponential-doping Ga_{0.37}Al_{0.63}As and uniform-doping GaAs.

3.3. Femto-second transient dynamics measurement

In the femtosecond ultrafast dynamics measurement experiment, the transient reflectivity rate of uniform-doping GaAs photocathode sample 1 and exponential-doping Ga_{0.37}Al_{0.63}As photocathode sample 3 is measured by pump-probe transient reflectivity system. The measurement results of transient rate of reflectivity of two photocathode samples are shown in Fig. 6.

As it can be seen from Fig. 6, it exhibits the relationship of transient reflectivity rate verse the delay time (ps) and shows the evolution process of carriers dynamics movement. There is a sharp rise of reflectivity in an ultra-short time about 2.5 ps to reach their maximum under femtosecond laser illumination. The peak value of sample 1 is higher than sample 1, the peak value of ΔR/R of uniform-doping sample 1 is about 1.74 × 10⁻⁴ and that of exponential-doping sample 3 is 2.74 × 10⁻⁴.

After reaching their peaks, the reflectivity of sample is gradually slowing down and the dropping speed of Ga_{0.37}Al_{0.63}As is slower than GaAs. Sample 1 exhibits faster relaxation with ΔR/R dropping to less than half of its peak within 50 ps. The reduction rate of ΔR/R is nearly a constant. However, sample 3 exhibits slower relaxation and we infer that the value of ΔR/R falling to half of its peak may take 250 ps. This difference between sample 1 and sample 3 could result from their different Al constituent content and different doping structure. The exponential-doping Ga_{0.37}Al_{0.63}As photocathode sample 3 leads to more electron population buildup near surface and longer carrier lifetime.

4. Discussion

The distinct between uniform-doping GaAs photocathode (sample 1) and exponential-doping GaAs photocathode (sample 2) is different doping structure. Quantum efficiency of sample 2 is higher than that of sample 1, which means exponential-method is better for performance of photocathode. Compared with Table 2, it proves the truth that performance parameters such as L_D, P and S_v of exponential-doping GaAs is higher than uniform-doping GaAs. It attributes to that exponential-doping contributes to forming built-in electric oriented from the top to bottom of emission layer. Oriented movement of carriers reduce the energy loss caused by carrier randomly crashing and scattering, resulting to more electrons possessing more energy to transfer to the surface and emit to vacuum. Small S_v also contributes to the improvement of escape probability P of electrons.

Finally, the transient reflectivity rate is measured by broadband pump-probe transient reflectivity system. From Fig. 6, we can observe the evolution process of carrier transient dynamics. The transient reflectivity rate ΔR/R is related to dielectric constant Eq. (1.4):

$$\frac{\Delta R}{R} = \frac{4n_0 \cos(\theta)}{(n^2 - 1)[n_0^2 - \sin^2(\theta)]^{1/2}} \Delta n \tag{1.4}$$

θ is incident angle of probe light, n is the real part of dielectric constant, n₀ = Re(ε^{1/2}), Δn = Δn_{FC} + Δn_{LT} + Δn_{SF}, Δn_{FC} represents contribution of free carriers, Δn_{LT} represents contribution of lattice temperature, Δn_{SF} represents contribution of state filling effect.

All behaviors in Fig. 6 indicate the process of carrier transportation. The initial sharp rise of transient reflectivity is due to that many photo-generated free electrons near surface are excited by pump light and they possess high energy. The amount of free carriers increasingly accumulates in an ultra-short time showing as a sharp rise of reflectivity. Meanwhile, the electrons in deeper emission layer are also excited and continually move to the surface, causing the continue rise of reflectivity. The ultra-short time of rising process keeps about 3 ps. Upon reaching their peak values, electrons saturation effect degrades and relaxation begins to dominate. Therefore, the transient reflectivity rate gradually decreases. The reduction rate of ΔR/R of sample 1 is faster than sample 3. This may be due to built-in electric field caused by exponential-doping (sample 3) and other multi-process taking place simultaneously counters the relaxation effect. Built-in electric field is able to promote deeper electrons inside photocathode move to surface and diffuse longer route (according to Table 2). This kind of behavior can weaken even counter the relaxation effect. However, the superior does not exist in uniform-doping photocathode (sample 1).

In Fig. 6, The transient reflectivity of Ga_{0.37}Al_{0.63}As is higher than GaAs, it may be not only attributed to the built-in electric field, but also may it attribute to the intrinsic property of materials. Another reason may attribute to a fact that the electron diffusion length (L_D) of Ga_{1-x}Al_xAs photocathode material is decreasing with the increasing of Al constituent [18]. The Al content in Ga_{0.37}Al_{0.63}As photocathode is higher than GaAs photocathode resulting to electrons in Ga_{0.37}Al_{0.63}As can diffuse longer distance and are more able

to move to the material surface.

Overall, the exponential-doping structures are more excellent than traditional uniform-doping structures in the terms of performance concerned. It is beneficial for improve quantum efficiency in some degree and transient carrier dynamics research is original compared with prior reports. In the area of transient detection, femtosecond method has a variable future. However, the current work on femtosecond measurement is not enough and it deserves more attention paying on it.

5. Conclusion

We research electronic and optical property of $\text{Ga}_{1-x}\text{Al}_x\text{As}$ with Al constituent $x = 0, 0.25, 0.63$ and 1 by means of GASTEP calculation. It is found that $\text{Ga}_{1-x}\text{Al}_x\text{As}$ varies from direct band gap to indirect band gap at $x = 0.45$. Adsorption peaks of $\text{Ga}_{1-x}\text{Al}_x\text{As}$ move to high energy side with the increasing of Al constituent. Exponential-doping method in GaAs photocathode is better to improve the performance and ability of photocathode than uniform-doping method. Exponential-doping method makes GaAs possess longer L_D , higher P and smaller S_V . It is mainly attributed to the built-in electric field. The transient rate of reflectivity on uniform-doping GaAs and exponential-doping $\text{Ga}_{0.37}\text{Al}_{0.63}\text{As}$ is measured by broadband pump probe transient reflectivity system, respectively. The results show that exponential-doping not only promote more electrons transition but also results in more electrons accumulation near surface. Moreover, transient dynamics phenomenon about carrier evolution process is presented by the system. However, relative research about transient dynamics on NEA photocathode is few and deeper research should be conducted and noted. The femtosecond transient measurement method is significant for the investigation and fabrication of GaAlAs photocathode in the future.

Acknowledgements

Thanks Meishan Wang of school of Information and Electrical Engineering, Ludong University for first principle calculations. This work was supported by the National Natural Science Foundation of China with grant No. 61775203, 61308089 and 6144005, the National Key Research & Development Plan Project No. 2017YFF0210800, Public Technology Applied Research Project of Zhejiang Province (No. 2013C31068).

References

- [1] F. Machuca, Y. Sun, Z. Liu, et al., *J. Vac. Sci. Technol. B* 18 (6) (2000) 3042–3046.
- [2] S. Karkare, L. Boulet, L. Cultrera, et al., *Phys. Rev. Lett* 097601 (2014) 112.
- [3] M.Z. Yang, B.K. Chang, W.F. Rao, *Optik* 127 (2016) 10710–10715.
- [4] J.W. Schwede, I. Bargatin, D.C. Riley, et al., *Nat. Mater.* 9 (2010) 762–767.
- [5] L. Chen, Y. Shen, S.Q. Zhang, Y.S. Qian, S.N. Xu, *Opt. Comm.* 355 (2015) 186–190.
- [6] T. Ohno, *Surf. Sci.* 357 (1996) 265–269.
- [7] R. Shirley, M. Kraft, *Phys. Rev. B* 81 (2010) 075111.
- [8] C. Hogan, D. Paget, Y. Garreau, M. Sauvage, G. Onida, et al., *Phys. Rev. B* 205313 (2003) 68.
- [9] J.P. Perdew, K. Burke, M. Ernzerhof, *Appl. Phys. Lett* 77 (18) (1996) 3865–3868.
- [10] H.J. Monkhorst, J.D. Pack, *Phys. Rev. B* 13 (12) (1976) 5186–5192.
- [11] X.L. Chen, M.C. Jin, Y.G. Zeng, G.H. Hao, Y.J. Zhang, B.K. Chang, F. Shi, H.C. Cheng, *Appl. Opt.* 153 (32) (2014).
- [12] X.Q. Du, B.K. Chang, *Appl. Surf. Sci.* 251 (2005) 267.
- [13] B.J. Stocker, *Surf. Sci.* 47 (1975) 501–513.
- [14] X.L. Chen, G.H. Hao, B.K. Chang, Y.J. Zhang, J. Zhao, Y. Xu, M.C. Jin, *Appl. Opt.* 52 (25) (2013).
- [15] S.L. Zhu, L. Chen, S.Q. Zhang, M.Y. He, L. Yin, Y.S. Qian, *Optik* 157 (2018) 968–957.
- [16] H. Jani, L. Chen, L.Z. Duan, *Proc. Of SPIE* 10530 (2018) 105300x-1.
- [17] X.H. Yu, Y.J. Du, B.K. Chang, Z.H. Ge, M.S. Wang, *Optik* 124 (2013) 4402–4405.
- [18] D.S. Jiang, D.X. Liu, Y.H. Zhang, H.L. Duan, R.H. Wu, *J. Semicond.* 13 (6) (1992) 333–336.
- [19] X.L. Chen, G.H. Hao, B.K. Chang, et al., *Appl. Opt.* 52 (25) (2013).